Surface Review and Letters, Vol. 16, No. 5 (2009) 749–755

World Scientific
www.worldscientific.com

THE CO-ADSORPTION OF BENZENE AND CO ON Co(0001)

ESTELA A. GONZÁLEZ, PAULA V. JASEN, JORGE PIERINI,
GRACIELA BRIZUELA and ALFREDO JUAN*
Departamento de Física, Universidad Nacional del Sur,
Av. Alem 1253, Bahía Blanca (8000), Argentina
**cajuan@uns.edu.ar*

Received 4 May 2009

The co-adsorption of carbon monoxide and benzene on Co(0001) has been studied using density functional calculations. We used the ordered $(\sqrt{7} \times \sqrt{7})$ $R19^\circ$ surface unit cell. A comparison of the co-adsorption with CO and benzene two-dimensional networks is also given. The electronic structure reveals that the CO orbitals interact with benzene and Co layer. Regarding the bonding, the Co–Co overlap population decrease 18% after benzene adsorption and increase a little after CO adsorption with a net 14.6% decrease in the co-adsorption system. The CO–benzene interaction is shown by the changes in the C–O (CO) and C–H (benzene) bonds.

Keywords: DFT; benzene; co-adsorption; electronic structure.

1. Introduction

The adsorption of benzene on metallic surfaces is of considerable interest because it serves as a model for other more complex systems. Benzene adsorbed easily on most transition metal surfaces[1] and the molecule acts as an electron donor. The bonding of aromatic hydrocarbons plays an important role in many catalytic processes. The adsorption geometry of the benzene molecule is hence of fundamental importance. The main issues being discussed in the past are the magnitude of substrate-induced distortions on the molecule and the effect of the neighboring molecules on the choice of the adsorption site and orientation.

The benzene/metal interaction has been studied on a large number of metal surfaces. An excellent review on these systems can be found in Refs. 1 and 2. In the case of cobalt, we can mention the adsorption of benzene on Co(10–10)[3,4] and W(110) supported Co(0001) films.[5]

The benzene molecule adsorbs on an hcp site with the two parallel C–C bonds aligned in [1–100] direction. The carbon–carbon bond distances remain at their gas phase value and only small buckling is observed in the carbon ring. Compared to other studies of benzene adsorption on close packed surfaces, the results indicate that the molecule is more loosely bounded to the Co{0001} surface than to the other close packed surfaces.[6]

On the other hand, the adsorption of CO on transition metal surfaces has been extensively studied for over 20 years with the aim of understanding the chemical bond of CO to the surface. However, studies on Co have been relatively rare compared with its neighbors in the Periodic Table[7–14] despite the importance of cobalt as a catalytic material. Cobalt is located at the border of molecular adsorption for CO[15] with its neighbors Ni and Fe clearly contrasted in their ability to dissociate CO.

*Corresponding author.

The adsorption site for CO is on top in most cases but on Ni(111) bridge sites[13] and Pd(111) fcc-hollow sites[9,10] have been observed. The adsorption of CO on Co(0001) has been experimentally studied and CO adsorbs only at on-top sites, independent of the amount of adsorbed CO.[16–19]

The co-adsorption of benzene with carbon monoxide has been studied on Ru(0001),[20,21] Pd(111),[22,23] Pt(111),[24,25] Ni(100) and Ni(111),[26–29] and Rh(111).[24,30–32]

Previous studies of benzene adsorption on Co(0001) showed that two different adsorption structures can be found, depending on the benzene amount and adsorption temperature. At low exposures (<20 L), a $c(2\sqrt{3}\times 4)$rect structure is observed. If the adsorption temperature is lower than 220 K, a $(\sqrt{7}\times\sqrt{7})\,R19°$ structure appears.[33] CO shows a re-ordering effect of benzene on Rh(111) and Ni(111).[26–28,30–32] These facts raise the question of whether CO co-adsorption also influences the ordered structures of benzene on Co(0001). The co-adsorption of CO and benzene enhances the understanding of the influence of an electron acceptor molecule on an electron donor molecule. A previous study showed that pure benzene decreased the work function of Co(0001).[33] Therefore, benzene can be seen as an electron donor for cobalt, while CO is known to act as an electron acceptor. This suggests an attractive interaction between co-adsorbed CO and benzene on Co(0001).

The benzene molecules are adsorbed flat on the surface at threefold hollow site except with high CO coverage where the adsorption site or the orientation of the benzene molecule is believed to change.[34] In conclusion, CO adsorption blocks the benzene adsorption by a factor of three on the surface. This is true for both pre-adsorbed CO, where blocking of benzene adsorption is detected, and post-adsorbed CO, where benzene desorption is induced. In both cases, however, some benzene is still left on the surface even at saturation CO exposures. The amount of desorbed hydrogen decreases as the CO exposure is increased. The reduction in the hydrogen desorption results from site blocking/induced desorption of C_6H_6 caused by CO. However, complete quenching is not observed. The data also suggests that the CO–benzene attraction remains small.

In this paper, we will study the co-adsorption of CO and benzene on Co(0001) using DFT calculations to reveal the electronic and bonding between co-adsorbates and the substrate.

2. Theoretical Method

All calculations described herein were performed within the framework of density functional theory (DFT) using a basis set consisting of plane waves, as implemented in the VASP code.[35–37] The electron–ion interactions were described by ultrasoft pseudopotentials,[38] and the exchange and correlation energies were calculated with the Perdew–Wang form of the generalized gradient approximation (GGA).[39] Spin-polarization and nonlinear core corrections[40] were included in the calculations for systems with Co to correctly account for its magnetic properties. Spin polarization has been shown to have a major effect on the adsorption energies for magnetic systems[41] and may alter the topology of the potential energy surfaces. Co is hexagonal close-packed metal, and the {0001} surface is the close-packed surface. In our calculations, the surface was modeled by a four-layer slab with one benzene molecule in the primitive $(\sqrt{7}\times\sqrt{7})\,R19°$ surface unit cell (see Fig. 1), separated by a vacuum region equivalent to six bulk metal layers. The one-sided slab has been used extensively in the literature and has been proven to be accurate.[42,43] A plane wave cutoff energy of 320 eV was used in the calculation, and the Brillouin zone of the surface unit cell was sampled with a $7\times7\times7$ Monkhorst–Pack mesh.[44] The adsorption energies were calculated taking the difference between the total adsorbate/surface system, and the individual surface and individual adsorbate. The calculated lattice constants in bulk Co $a = 2.53$ Å and $c/a = 1.27$ Å compare well with the experimental values. The computed magnetic moment was 1.63.[45]

To understand the Co–C_6H_6–CO interactions, we used the concept of density of states (DOS) and overlap population density of states (OPDOS). The DOS curve is a plot of the number of orbitals as a function of the energy. The integral of the DOS curve over an energy interval gives the number of one-electron states in that interval; the integral up to the Fermi level (E_F) gives the total number of occupied molecular orbitals. If the DOS is weighed with the overlap population between two atoms, the OPDOS is obtained. The integration of the OPDOS curve up to E_F gives the total overlap population of the

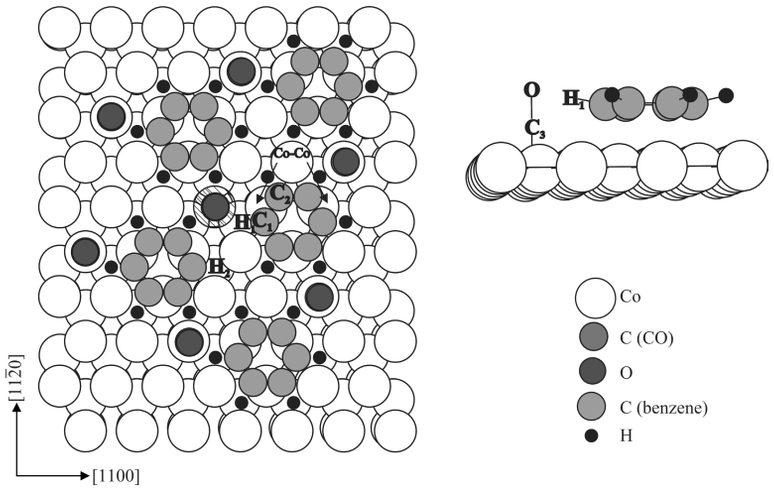

Fig. 1. Schematic view of $(C_6H_6)_5$–$(CO)_7$/Co system, frontal on the left and lateral on the right.

specified bond orbital and it is a measure of the bond strength. If an orbital at certain energy is strongly bonded between two atoms, the overlap population is strongly positive and OPDOS curve will be large and positive around that energy. Similarly, OPDOS is negative around certain energy and this corresponds to antibonding interactions. The OPDOS curves were computed using the YAeHMOP code.[46]

We used the experimental adsorption geometry determined by Habermehl-Cwirzen *et al.*[34] The carbon monoxide molecules were taken to stand perpendicular to the surface on top-sites ring and buckling distortions were also considered. The computed H-ring angle was 12.0°.

The average perpendicular distance between the aromatic ring and the first Co layer was 2.321 Å. The shortest Co–Co bond distance was 2.507 Å. Carbon–hydrogen bond distances were almost the same to that in the gas phase benzene. The Co interlayer spacing remained similar to the bulk value.

3. Results and Discussion

The results for the clean Co(0001) surface is presented in Table 1. The computed Co orbital population is $s^{0.63}\ p^{0.24}\ d^{7.95}$ with an overlap population (OP) of 0.205. The width of the d band is approximately 5 eV (see Fig. 2). This value is in agreement with data in the literature.[47] The dispersion of the s and p bands is much larger than that of the d band, reflecting the much more contracted nature of d orbitals.

Table 1. Electron density, overlap population (OP), charge and distances for a Co, a (C_6H_6) and a (CO) cluster.

	Electron orbital occupation					
Structure	s	p	d	Bond type	OP	Distance (Å)
Co						
Co	0.63	0.24	7.95	Co–Co	0.205	2.507
$(C_6H_6)_5$ vacuum						
H	0.78	0.00	0.00	H–H	0.014	2.507
C	0.92	1.21	0.00	C–C	0.647	1.395
				C–H	0.637	1.139
$(CO)_7$ vacuum						
C	0.43	0.33	0.00	C–O	0.798	1.170
O	1.62	3.31	0.00			

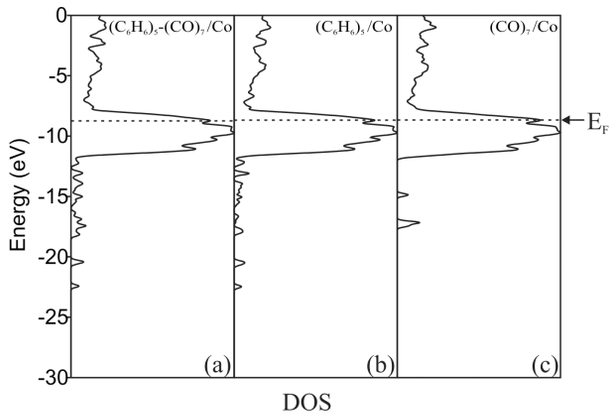

Fig. 2. Total DOS curves for $(C_6H_6)_5$–$(CO)_7$/Co (a), $(C_6H_6)_5$/Co (b), and $(CO)_7$/Co (c).

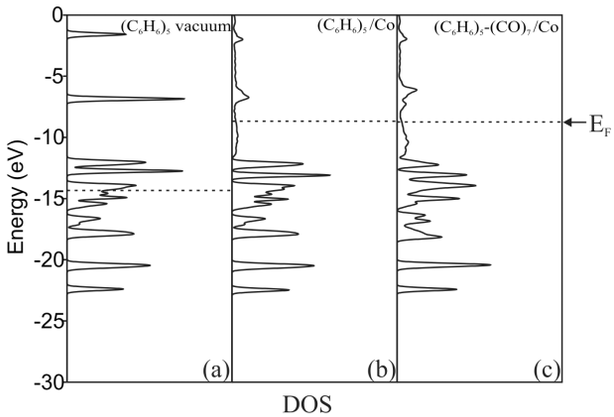

Fig. 3. Total DOS curves for $(C_6H_6)_5$ in vacuum (a), a $(C_6H_6)_5$/Co (b), and a $(C_6H_6)_5$–$(CO)_7$/Co (c) projected DOS on benzene.

The total DOS of the co-adsorption system presents a small peak below −20 eV belonging to the benzene ring (see Fig. 2(b)) and two peaks at −17.16 and −14.87 eV related to carbon monoxide (Fig. 2(c)).

Figures 3 and 4 show the projected DOS (PDOS) of benzene and CO in vacuum, adsorbed and as a part of the co-adsorbed system. If we compare Fig. 3(a) with (b), there is almost no change in the DOS. Thus, a relatively weak interaction between the cobalt substrate and the carbon ring in the benzene can be predicted. The same result was reported by Pussi *et al.*[6]

In the case of CO adsorption, the interaction with the metal surface is noticeable (compare Fig. 4(a) with (b) and (c)). When a monolayer of CO is

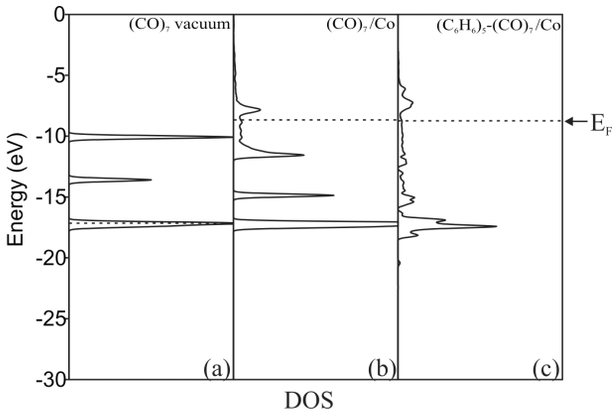

Fig. 4. Total DOS curves for $(CO)_7$ in vacuum (a), a $(CO)_7$/Co (b), and a $(C_6H_6)_5$–$(CO)_7$/Co (c) projected DOS on carbon monoxides.

considered, the peak at −10 eV becomes hybridized with the metal orbitals in the range $(-8, -12)$ eV while the peak at −13.6 eV is shifted to −15 eV.

The coadsorbed system shows an interaction between benzene and carbon monoxide (compare Figs. 3(c) and 4(c)) more important than between benzene and the Co substrate.

The PDOS of carbon monoxide in Fig. 3(c) shows that all valence orbitals of CO are interacting with benzene and the Co layer. The broadening of the band at −17.9 eV supports the idea of a CO–benzene interaction.

The electron orbital occupation, overlap population and distances are shown in Tables 1–3. In the $(C_6H_6)_5$–CO_7/Co system (see Table 3), the C_1–C_2, C_1–H_1 and Co–C_1 bond distances are close to the values determined by LEED.[6]

Regarding the bonding, the metal–metal bond OP decreases 18% after benzene adsorption and increases a little after CO adsorption (3.4%) while in the coadsorbate system it decreases (14.6%). The C_1–C_2 OP increases on the surface with or without CO when it is compared to a hypothetical $(C_6H_6)_5$ network in vacuum (68 and 68.3%, respectively). Figures 5(d)–5(f) also show that more bonding states are populated above −15 eV.

A similar behavior is observed for the C_1–H_1 bond. As the Fermi level (E_F) shift to higher values, more bonding states are populated. The H–H interaction is null indicating that benzene–benzene interaction is not relevant.

Table 2. Electron density, overlap population (OP), charge and distances for a $(C_6H_6)_5$/Co and a $(CO)_7$/Co cluster.

Structure	Electron orbital occupation			Bond type	OP	Distance (Å)
	s	*p*	*d*			
Co–$(C_6H_6)_5$						
Co	0.49	0.25	7.16	Co–Co	0.168	2.507
H	1.03	0.00	0.00	H_1–H_2	0.002	2.507
C	0.95	3.09	0.00	C_1–C_2	1.087	1.395
				Co–H_1	0.000	2.827
				Co–C_1	0.125	2.321
				C_1–H_1	0.871	1.140
Co–$(CO)_7$						
Co	0.62	0.23	7.72	Co–Co	0.212	2.507
C	1.13	3.56	0.00	C_3–O	0.590	1.170
O	1.63	5.78	0.00			
Co	0.56	0.48	6.22	Co–C_3	1.071	1.780
				Co–O	0.000	2.950

Table 3. Electron density, overlap population (OP), charge and distances for a $(C_6H_6)_5$–$(CO)_7$/Co cluster.

Structure	Electron orbital occupation			Bond type	OP	Distance (Å)
	s	*p*	*d*			
Co–$(C_6H_6)_5$–$(CO)_7$						
Co	0.48	0.25	7.03	Co–Co	0.175	2.507
$H_{C_6H_6}$	0.86	0.00	0.00	H_1–H_2	0.000	2.507
$C_{C_6H_6}$	0.98	3.14	0.00	C_1–C_2	1.089	1.395
				C_1–H_1	0.834	1.140
				Co–C_1	0.126	2.321
				Co–H_1	0.000	2.827
C_{CO}	1.03	2.38	0.00	C_3–O	0.730	1.170
O_{CO}	1.55	4.51	0.00	C_1–C_3	0.000	2.512
				C_1–O	0.000	2.588
				C_3–H_1	0.058	1.586
				O–H	0.000	1.546
	0.56	0.45	6.79	Co–C_3	1.057	1.780
				Co–O	0.000	2.950

The most revealing information of the molecular interaction comes from the changes in the carbon monoxide molecule. Adsorbed on pure Co, the C–O OP decreases 26%. When benzene is co-adsorbed, the OP approaches to its original values (0.730 vs 0.798, see Tables 3 and 1). This can be seen in Figs. 5(g)–5(i). The C_3–O bond has an antibonding interaction at -10 eV that is not populated in the free molecular network.

When the CO lattice is adsorbed on Co (Fig. 5(g)), the -10 eV peak hybridizes with the *d* metal band in the range $(-12, -8)$ eV (Fig. 5(h)) and as the antibonding states populate, the OP decreases. When benzene is co-adsorbed, an intermolecular interaction brings more bonding states that comes from benzene through the moving metal matrix (Fig. 5(i)). At the same time, the C_3-metal OP does not change its net value in the coadsorbate

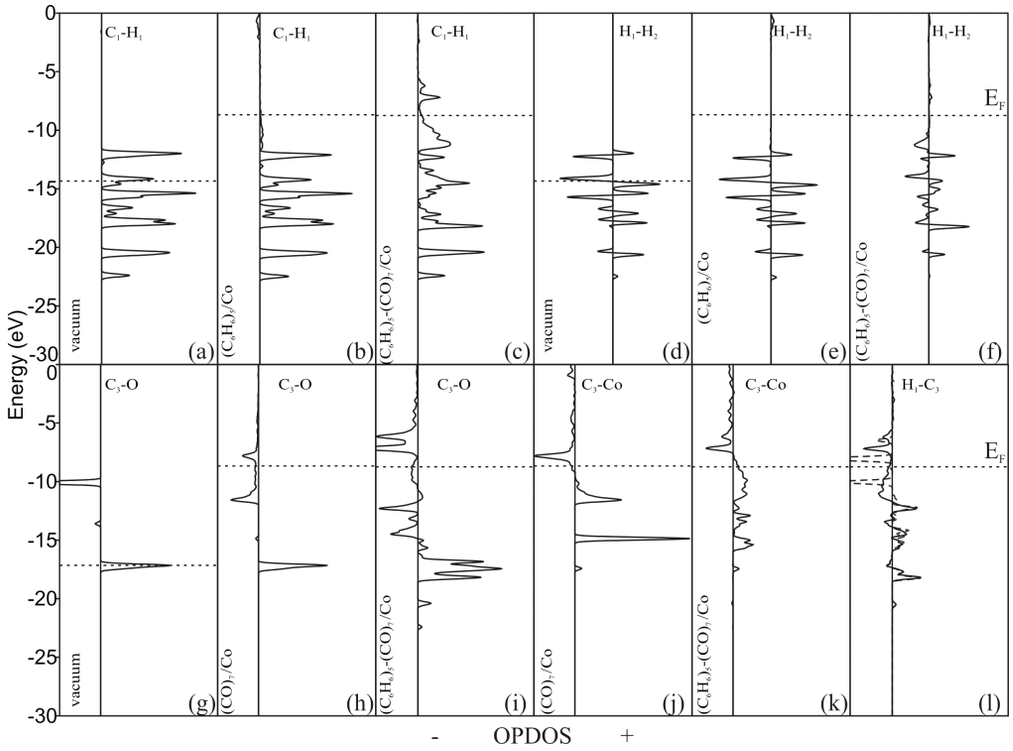

Fig. 5. OPDOS curves for: C_1–H_1 bond in vacuum (a), in $(C_6H_6)_5$/Co (b) and in $(C_6H_6)_5$–$(CO)_7$/Co (c), C_1–C_2 bond in vacuum (d), in $(C_6H_6)_5$/Co (e) and in $(C_6H_6)_5$–$(CO)_7$/Co (f), C_3–O bond in vacuum (g), in $(CO)_7$/Co (h) and in $(C_6H_6)_5$–$(CO)_7$/Co (i), C_3–Co bond in $(CO)_7$/Co (j) and in $(C_6H_6)_5$–$(CO)_7$/Co (k), H_1–C_3 bond in $(C_6H_6)_5$–$(CO)_7$/Co (right line) and in vacuum (dashed line) (l).

system; however, the orbital contributions are much more hybridized in the $(-17, E_F)$ eV range (see Figs. 5(j) and 5(k)).

The benzene–CO interaction is also revealed following the H_1–C_3 OP. In a hypothetical CO–benzene network in vacuum, its value is 0.099, when coadsorbed changes to 0.058.

4. Conclusions

We analyzed the CO–benzene co-adsorption on Co(0001). Starting from experimental information, we have computed the C–H ring angle of 12.0°. The DOS plots show that the CO–benzene interaction is weak; however, it is more important than those in the isolated adsorbed system. The metal–metal bond overlap population (OP) decreases while the C–C bond OP within the benzene ring increases with or without CO on Co. On the other hand, CO presents a bigger change hybridizing its orbitals on the Co(0001) layer.

Acknowledgments

Our work was supported by SGCyT Universidad Nacional del Sur and PICT 1186. A. Juan, G. Brizuela, E. A. González and P. V. Jasen are members of CONICET.

References

1. G. A. Somorjai, *Introduction to Surface Chemistry and Catalysis* (Wiley-Interscience Publication, 1994).
2. H.-P. Steinbrueck, W. Huber, T. Pache and D. Menzel, *Surf. Sci.* **218** (1989) 293.
3. K. Pussi, M. Lindroos and C. J. Barnes, *Chem. Phys. Lett.* **341** (2001) 7.
4. C. J. Barnes, M. Valden and M. Pessa, *Surf. Rev. Lett.* **7** (2000) 67.
5. M. Getzlaff, J. Bansmann and G. Schonhense, *Surf. Sci.* **323** (1995) 118.
6. K. Pussi, M. Lindroos, J. Katainen, K. Habermehl-Cwirsen, J. Lahtinen and A. P. Seitsonen, *Surf. Sci.* **572** (2004) 1.

7. G. Michalk, W. Moritz, H. Pfnür and D. Menzel, *Surf. Sci.* **129** (1983) 92.
8. H. Over, W. Moritz and G. Ertl, *Phys. Rev. Lett.* **70** (1993) 315.
9. M. Gierer, A. Barbieri, M. A. Van Hove and G. A. Somorjai, *Surf. Sci.* **391** (1997) 176.
10. T. Giessel, O. Schaff, C. J. Hirschmugl, V. Fernandez, K.-M. Schindler, A. Theobald, S. Bao, R. Lindsay, W. Berndt, A. M. Bradshaw, C. Baddeley, A. F. Lee, R. M. Lambert and D. P. Woodruff, *Surf. Sci.* **406** (1998) 90.
11. H. Ohtani, M. A. Van Hove and G. A. Somorjai, *Surf. Sci.* **187** (1987) 372.
12. D. F. Ogletree, M. A. Van Hove and G. A. Somorjai, *Surf. Sci.* **173** (1986) 351.
13. S. D. Kevan, R. F. Davis, D. H. Rosenblatt, J. G. Tobin, M. G. Mason, D. A. Shirley, C. H. Li and S. Y. Tong, *Phys. Rev. Lett.* **46** (1981) 1629.
14. E. J. Moler, S. A. Kellar, W. R. A. Hyff and Z. Hussain, *Phys. Rev. B* **54** (1996) 10862.
15. G. Broden, T. N. Rhodin, C. Bruckner, R. Benbow and Z. Hurych, *Surf. Sci.* **59** (1976) 593.
16. M. E. Bridge, C. M. Comrie and R. M. Lambert, *Surf. Sci.* **67** (1977) 393.
17. J. Lahtinen, J. Vaari and K. Kaurala, *Surf. Sci.* **418** (1998) 502.
18. H. Papp, *Surf. Sci.* **129** (1983) 205.
19. F. Greuter, D. Heskett, E. W. Plummer and H.-J. Freund, *Phys. Rev. B* **27** (1983) 7117.
20. P. Jakob and D. Menzel, *Surf. Sci.* **235** (1990) 15.
21. P. A. Heimann, P. Jakob, T. Pache, H.-P. Steinbrueck and D. Menzel, *Surf. Sci.* **210** (1989) 282.
22. H. Ohtani, M. A. Van Hove and G. A. Somorjai, *J. Phys. Chem.* **92** (1988) 3974.
23. H. Ohtani, B. E. Bent, C. M. Mate, M. A. Van Hove and G. A. Somorjai, *Appl. Surf. Sci.* **33/34** (1988) 254.
24. C. M. Mate and G. A. Somorjai, *Surf. Sci.* **160** (1985) 542.
25. P. V. Jasen, G. Brizuela, Z. Padín, E. A. González and A. Juan, *Appl. Surf. Sci.* **236** (2004) 394.
26. P. M. Blass, S. Akhter and J. M. White, *Surf. Sci.* **191** (1987) 406.
27. H.-P. Steinbrueck, W. Huber, T. Pache and D. Menzel, *Surf. Sci.* **218** (1989) 293.
28. W. Huber, P. Zebisch, T. Bornemann and H.-P. Steinbrueck, *Surf. Sci.* **258** (1991) 16.
29. W. Huber, H.-P. Steinbrueck, T. Pache and D. Menzel, *Surf. Sci.* **217** (1989) 103.
30. E. Bertel, G. Rosina and F. P. Netzer, *Surf. Sci.* **172** (1986) L515.
31. M. A. Van Hove, R. F. Lin and G. A. Somorjai, *J. Am. Chem. Soc.* **108** (1986) 2532.
32. R. F. Lin, G. S. Blackman, M. A. Van Hove and G. A. Somorjai, *Acta Cryst. B* **43** (1987) 368.
33. K. Habermehl-Cwirzen, J. Katainen, J. Lahtinen and P. Hautojärvi, *Surf. Sci.* **507–510** (2002) 57.
34. K. Habermehl-Cwirzen, J. Lahtinen and P. Hautojärvi, *Surf. Sci.* **584** (2005) 70.
35. G. Kresse and J. Hafner, *Phys. Rev. B* **47** (1993) 558.
36. G. Kresse and J. Furthmüller, *Phys. Rev. B* **54** (1996) 11169.
37. G. Kresse and J. Furthmüller, *Comput. Mater. Sci.* **6** (1996) 15.
38. D. Vanderbilt, *Phys. Rev. B* **41** (1990) 7892.
39. J. Perdew, J. A. Chevary, S. H. Vosko, K. A. Jackson, M. R. Pederson, D. J. Singh and C. Fiolhais, *Phys. Rev. B* **46** (1992) 6671.
40. S. G. Louie, S. Froyen and M. L. Cohen, *Phys. Rev. B* **26** (1982) 1738.
41. Q. Ge, S. S. Jenkins and D. A. King, *Chem. Phys. Lett.* **327** (2000) 125.
42. B. Hammer and J. K. Nørskov, *Adv. Catal.* **45** (2000) 71.
43. Q. Ge, R. Kose and D. A. King, *Adv. Catal.* **45** (2000) 207.
44. H. J. Monkhorst and J. D. Pack, *Phys. Rev. B* **13** (1976) 5188.
45. C. Kittel, *Introduction to Solid State Physics*, 7th edn. (Wiley, New York, 1996).
46. G. Landrum and W. Glassey, *Yet Another Extended Hückel Molecular Orbital Package (YAeHMOP)* (Cornell University, 2001), http://overlap.chem.cornell.edu:8080/yahemop.html.
47. R. Griessen, *Phys. Rev. B* **38** (1988) 3690.

October 23, 2009 17:42 01310